NANO LETTERS

2008
Vol. 8, No. 12
4534-4538

Modal Characteristics in a Single-Nanowire Cavity with a Triangular Cross Section

Min-Kyo Seo,[†] Jin-Kyu Yang,[†] Kwang-Yong Jeong,[†] Hong-Gyu Park,[‡,*] Fang Qian,[§] Ho-Seok Ee,[‡] You-Shin No,[‡] and Yong-Hee Lee[†]

Department of Physics, Korea Advanced Institute of Science and Technology, Daejeon 305-701, Korea, Department of Physics, Korea University, Seoul 136-701, Korea, and Department of Chemistry and Chemical Biology, Harvard University, Cambridge, Massachusetts 02138

Received September 7, 2008

ABSTRACT

In this study, the modal characteristics of a single-GaN nanowire cavity with a triangular cross section surrounded by air or located on a silicon dioxide substrate have been analyzed. Two transverse resonant modes, transverse electric-like and transverse magnetic-like modes, are dominantly excited for nanowire cavities that have a small cross-sectional size of <300 nm and length of 10 μm. Using the three-dimensional finite-difference time-domain simulation method, quality factors, confinement factors, single-mode conditions, and far-field emission patterns are investigated for a nanowire cavity as a function of one length of the triangular cross section. The results of these simulations provide information that will be vital for the design and development of efficient nanowire lasers and light sources in ultracompact nanophotonic integrated circuits.

Active semiconductor nanowires with direct band gaps are widely employed for potential photonic applications.[1−11] For instance, low-threshold lasers,[1−6] multicolor light-emitting diodes (LEDs),[7] and low-loss active waveguides[8] have been successfully demonstrated using GaN or CdS nanowires. Among all potential nanoscale photonic light sources, nanowire lasers are particularly promising because a chemically synthesized single nanowire can naturally form a one-dimensional (1-D) Fabry−Perot cavity using clear end facets. Nanowire cavities typically have a small size with diameters ranging from 20 to 200 nm and lengths ranging from 2 to 40 μm and a large refractive index contrast for strong light confinement.[12] In addition to the experimental demonstration of various semiconductor nanowire lasers, optical properties such as quality (Q) factors,[13] reflectivities,[14] far-field emissions,[13] and lasing thresholds[15,16] have also been theoretically characterized. However, in these analyses all the nanowires were assumed to be dielectric cylinders with circular cross sections. In fact, nanowires can have various geometric cross sections, since the geometric cross section depends on the nanowire growth directions. For example, the cross section of a GaN nanowire can be triangular or hexagonal when the nanowire is grown along ⟨11−20⟩ or ⟨0001⟩ directions, respectively.[3,6,7] Therefore, when comparing measured optical properties with simulation results, one should obviously consider the geometric shapes of the actually synthesized nanowires.

Of the various semiconductor nanowires, GaN and InGaN nanowires have many practical advantages for use as an efficient light source in a nanophotonic integrated circuit.[7,10] These advantages include highly reproducible preparation with the n- and p-type doping, which is required for active, electrically driven photonic devices, and the emission wavelength can be tuned through variations in alloy composition of GaN. In this Letter, we investigate the optical characteristics of a single-GaN nanowire with a triangular cross section through theoretical analysis. Three-dimensional (3-D) finite-difference time-domain (FDTD) simulation[17] was performed to compute Q factors, confinement factors, single-mode conditions, and far-field emission patterns in a GaN nanowire cavity that is surrounded by air or located on a silicon dioxide (SiO_2) substrate. The novel simulation performed in such a realistic nanowire cavity structure can provide optimized structural parameters for the development of an efficient single-GaN nanowire laser with a low threshold. Furthermore, the FDTD results can be directly compared with measurements without unnecessary assumptions.

* Corresponding author, hgpark@korea.ac.kr.
[†] Korea Advanced Institute of Science and Technology.
[‡] Korea University.
[§] Harvard University.

10.1021/nl8027125 CCC: $40.75
Published on Web 11/05/2008

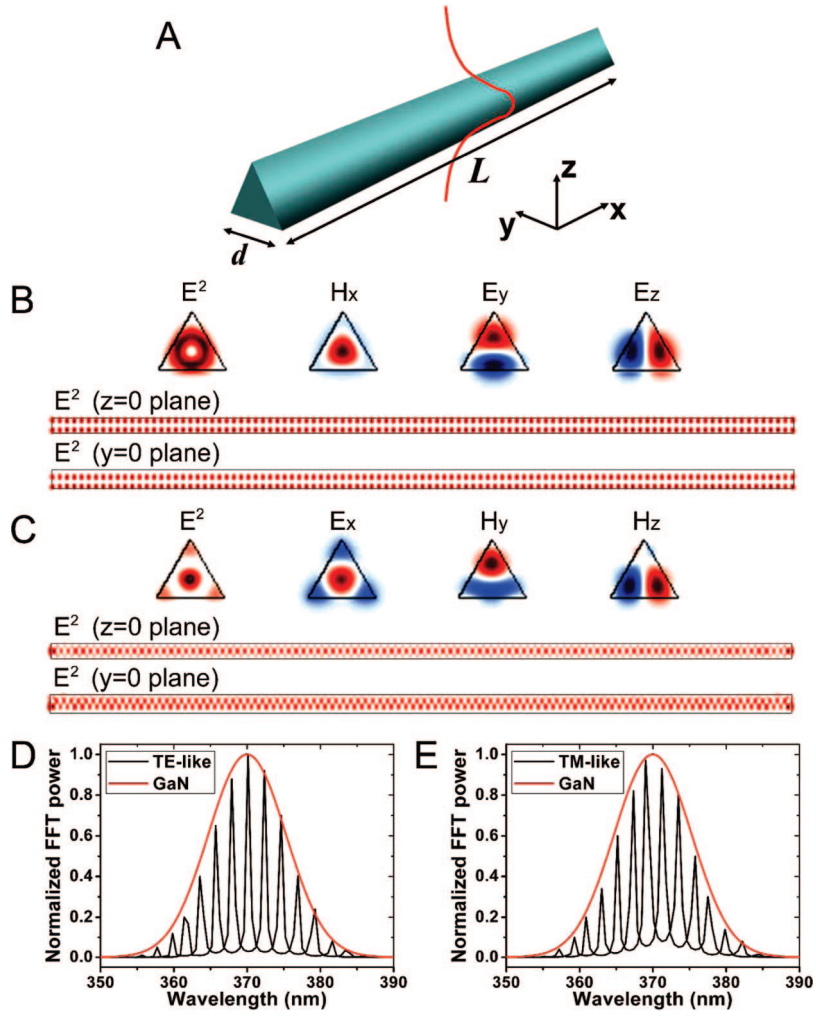

Figure 1. Modal characteristics of a free-standing single-GaN nanowire cavity at $d = 300$ nm. (A) Schematic illustration of a nanowire cavity with a triangular cross section. The nanowire axis is in the x-direction and the centroid of the cross section is the origin of the yz-plane. Electric and magnetic field components of (B) the TE-like and (C) the TM-like modes are computed by a 3-D FDTD simulation. Longitudinal mode spectra of (D) the TE-like and (E) the TM-like modes are also shown. Red lines are emission spectra of GaN.

Figure 1A shows a schematic illustration of a single-GaN nanowire cavity with a triangular cross section. In the simulation, the domain size was $15.0 \times 1.8 \times 1.8$ μm^3 and the grid size was 7.5 nm. The refractive index of GaN and the length of the nanowire, L, were set to 2.6 and 10 μm, respectively.[6] The length of the triangular nanowire cross section, d, was varied from 175 to 300 nm. The central emission wavelength of GaN was 370 nm, and the full width at half-maximum (fwhm) was 15 nm (red lines in Figure 1, panels D and E). The values used in this simulation were based on experimental measurements in a synthesized GaN nanowire.[6]

Simulations were conducted by first considering a free-standing GaN nanowire cavity surrounded by air (Figure 1). In FDTD simulations, resonant modes were excited by initial dipole sources located in the nanowire and then the simulation stored the time evolution of the electric and magnetic fields. The FDTD simulations demonstrated that two transverse modes were dominantly excited in the nanowire cavity when d was less than 300 nm (Figure 1, panels B and C). Each resonant mode was separately observed by an appropriate excitation source. One mode was solely excited by a dipole source with an H_x-field component (Figure 1B) and the other was excited by a dipole source with an E_x-field component (Figure 1C). Parts B and C of Figure 1 show the computed electric and magnetic field components of the resonant modes in a nanowire cavity with $d = 300$ nm. In the cross-sectional view of Figure 1B ($x = 0$ plane), only H_x, E_y, and E_z field components were dominantly observed, while the intensities of the other components were extremely weak. This electromagnetic pattern was indicative of a transverse-electric-like (TE-like) mode observed in a typical slab waveguide structure.[18] On the other hand, the transverse mode of Figure 1C, which has the dominant field components of E_x, H_y, and H_z, was indicative of a transverse-magnetic-like (TM-like) mode. The TE-like and the TM-like modes have distinguishable electric field intensity (E^2) distributions. The TE-like mode has an intensity node at the center, whereas the TM-like mode has a central intensity antinode at the center. This property was also clearly observed in the $z = 0$ and $y = 0$ planes, as shown in Figure 1, panels B and C. For both transverse modes, the time evolution of the fields was Fourier transformed to convert the field components to the frequency domain. As a result, 1-D Fabry−Perot

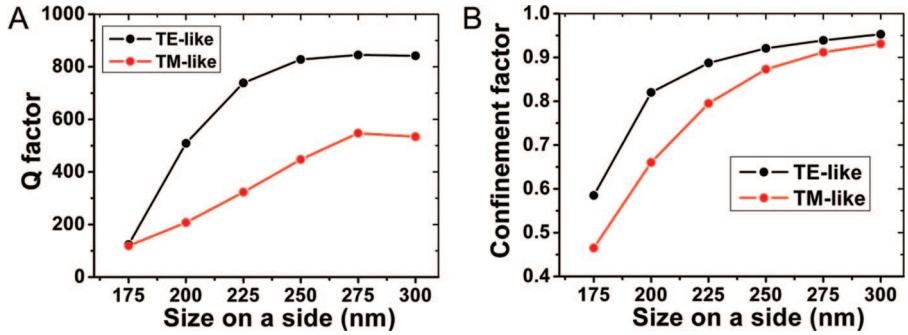

Figure 2. Q and confinement factors of the TE-like and the TM-like modes in a free-standing nanowire cavity. (A) Q factor vs nanowire size on a side. (B) Confinement factor vs nanowire size on a side.

resonances were observed for the field amplitude as a function of wavelength at $d = 300$ nm and $L = 10$ μm (Figure 1, panels D and E). The longitudinal mode spacing in each transverse mode was 2.24 nm, which agreed with the value obtained from the equation, $\Delta\lambda = \lambda^2/2nL$, where $\lambda = 370$ nm, $n = 2.6$, and $L = 10$ μm.[3,6] In addition, the longitudinal resonance peaks of the TE-like mode did not overlap with the peaks of the TM-like mode and hence the mode spacing between two longitudinal resonances was 1.12 nm if a diversity of the transverse mode was not considered.

To further understand the effect of a triangular cross section in the nanowire cavity, Q factors of the fundamental TE-like and TM-like resonant modes in a free-standing single-GaN nanowire cavity were calculated as a function of one length of the cross section, d (Figure 2A). The Q factor of the TE-like mode was almost two times higher than that of the TM-like mode at each d (>200 nm). The highest Q factors of the TE-like and TM-like modes were 840 and 530, respectively. Photons of the TE-like mode were effectively confined by the successful index guiding at each side of the triangular nanowire cross section as shown in the field profile, thus the TE-like modes have higher Q factors. However, the TM-like modes that have intensity antinodes at three sharp corners of the cross section had more optical losses (Figure 1C). Figure 2A also shows that the Q factors for both the transverse modes were saturated at $d >$ 275 nm. This occurred because sidewall loss is small and saturated in the nanowire cavity with a large diameter. In addition, higher-order transverse modes with higher Q factors started to appear in this region of d.[19]

The Q factors of the nanowire cavity computed in Figure 2A were relatively low compared to other nanocavities such as photonic crystals[20] and microdisks,[21] due to the smaller cavity size. Despite the fact that the Q factor of the nanowire cavity is <800, lasing can still be achieved in such a low-Q structure by confining light in the high refractive index of the semiconductor material. Lasing in the GaN nanowire cavity with a low-Q factor has been previously reported.[3,6] In these studies, a large confinement factor was responsible for the successful demonstration of lasing in a low-Q nanowire cavity. In general, the lasing threshold is proportional to $\exp(1/Q{\cdot}\Gamma)$, where Q is the Q factor and Γ is the confinement factor of a lasing mode.[22] Both high Q and large Γ values will lower the lasing threshold.[11] The confinement factor of a free-standing GaN nanowire was computed as a function of d using the FDTD method (Figure 2B). It is worth noting that large confinement factors (>0.9) were obtained for both transverse modes at $d >$ 275 nm.

With the Q factors and the confinement factors determined through the FDTD simulations in combination with the rate equations analysis, the relative lasing thresholds in the nanowire cavities with different diameters were investigated. The carrier density, N, and photon density, P, in the cavity can be described by following conventional rate equations in the case of optical pumping:[19,22]

$$\frac{dN}{dt} = \eta_i \frac{L_{in}}{\hbar\omega_p V} - (AN + BN^2 + CN^3) - \Gamma g(N)P$$

$$\frac{dP}{dt} = \Gamma g(N)P - \frac{P}{\tau_p} + \beta BN^2$$

where L_{in} is the pump power, η_i is absorbed ratio in active materials, ω_p is the frequency of a pumping laser, A is the surface nonradiative recombination coefficient, B is the radiative recombination coefficient, C is the Auger nonradiative recombination coefficient, Γ is the confinement factor, V is the active volume, and β is spontaneous emission factor. The photon lifetime, τ_p, is represented by $\tau_p = \lambda Q/2\pi c$, where λ is the wavelength of the output laser and Q is the Q factor of a resonant mode.[19] By use of previously determined material parameters of GaN[23] the optical gain was calculated by $g(N) = g_0 (c/n_{eff}) (N - N_{tr})$, where $g_0 = 2.5 \times 10^{-16}$ cm^2 and $N_{tr} = 7.5 \times 10^{18}$ cm^{-3}, and A, B, and C were 1×10^8 s^{-1}, 1.5×10^{-11} cm^3/s, and 1.4×10^{-31} cm^6/s, respectively. By use of an absorption coefficient of GaN, $\alpha \sim 170000$ cm^{-1}, at 266 nm,[24] the wavelength of a typical optical pumping laser, $\eta_i >\sim 0.7$, was computed. In addition, Q and confinement factors obtained by FDTD simulations (Figure 2) were considered. The rate equation analysis shows that, for example, the threshold of the TE-like mode at $d =$ 175 nm was approximately 3.1 times larger than the threshold of the TE-like mode at $d = 300$ nm (see Supporting Information, Figure S1). Although the Q factor at $d = 175$ nm is 6.8 times smaller than that at $d = 300$ nm, the threshold difference between the two cases was relatively small due to the large confinement factor and smaller active volume of the low-Q mode. Therefore, a large confinement factor was required to achieve low-threshold lasing in the nanowire cavity. Recently, synthesis of a GaN core/InGaN multiquantum wells (MQWs) shell nanowire heterostructure has been reported.[25] This structure, which consists of an active shell layer with a larger refractive index and lower-index nanowire core, could potentially have both large Q and confinement

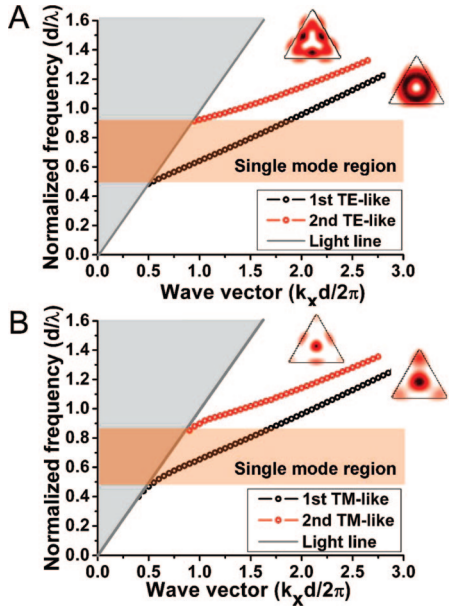

Figure 3. Dispersion curves of a free-standing nanowire cavity. Single-mode regions are shown in (A) the TE-like and (B) the TM-like modes.

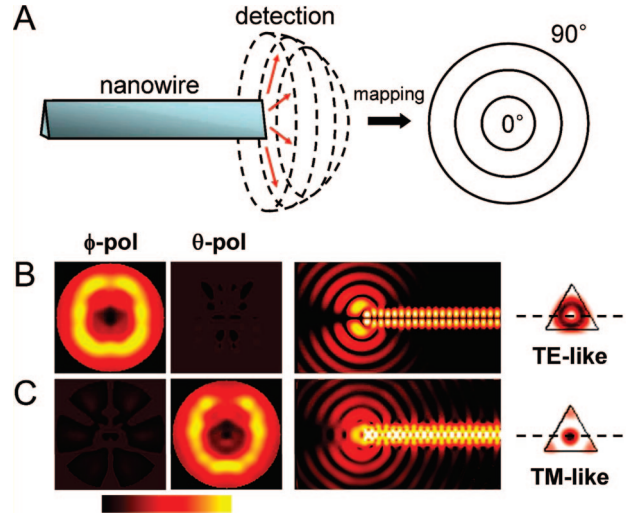

Figure 4. Far-field emission patterns from a free-standing single-GaN nanowire cavity. (A) Schematic illustration of the mapping procedure of a 3-D far-field emission pattern on to a 2-D plane. (B), (C) Far-field emission patterns at *yz*-planes (left two columns) and *xy*-planes (middle column) of the TE-like and the TM-like modes are computed, respectively. Right columns indicate respective near-field images. The left two columns show the polarization-resolved emission patterns of the modes.

factors because the TE-like mode with an intensity antinode in the shell would be dominantly excited. On the basis of our FDTD simulation and rate equation analysis, such a nanowire MQWs structure would provide a high material gain and, thus, would be advantageous in demonstrate lasing with a low threshold.[25]

In order to study single-mode conditions in the nanowire cavity, dispersion curves of the TE-like and the TM-like modes were plotted (Figure 3). A thick nanowire allows higher-order transverse modes as well as the fundamental mode and a thin nanowire allows only the fundamental mode. To calculate the dispersion curves, we used 3-D FDTD simulations with a periodic boundary condition in the *x*-direction instead of a perfectly matched layer (PML) boundary condition used for the simulations of Figures 1 and 2.[17] In Figure 3A, the normalized frequency, d/λ, of the TE-like mode in a free-standing GaN nanowire cavity was plotted as a function of the wave vector. The single TE-like mode was observed when d/λ varied from 0.5 to 0.9. When the wavelength λ was 370 nm, the corresponding d to this single-mode condition varied from 179 to 338 nm. When d was smaller than 179 nm, the mode was very close to the light line and hence the nanowire was unable to efficiently confine light. This strongly agrees with the simulation results shown in Figure 2A. However, in the case of the TM-like mode (Figure 3B), the single-mode condition was obtained when d varied from 162 to 315 nm at $\lambda = 370$ nm. Thus, if $d < 179$ nm, only the TM-like mode with a central intensity antinode was excited in the nanowire. In thicker nanowires ($d > 179$ nm), the TE-like modes would be dominant due to their higher Q and confinement factors. The dispersion curves determined in this study are necessary for the design of an efficient nanowire cavity that supports a desired transverse mode.

The study of far-field emission is generally useful in identifying and understanding the optical characteristics of a resonant mode excited in a cavity. In fact, it is not experimentally straightforward to clearly distinguish one mode from the others in a nanocavity through near-field images, such as panels B and C of Figure 1, due to the lack of a high-resolution measurement system. Even in the case of low-imaging resolution, far-field emission patterns can provide clear information for mode identification and can be accurately compared with measured properties.[26−28] Furthermore, the coupling efficiency of a resonant mode with a conventional optical fiber can be improved by analyzing the far-field emission.[28] By use of the near-field distribution at the surface of the nanowire cavity, the far-field emission profiles were computed (Figure 4A).[29] In addition, the polarization-resolved far-field emission patterns of the TE-like and the TM-like modes were computed (Figure 4, panels B and C, respectively). Note that both transverse modes were clearly distinguishable by the observation of polarization. The TE-like mode was completely polarized along the azimuthal direction (ϕ-polarized), while the TM-like mode was completely polarized along the zenithal direction (θ-polarized). These results can clearly be observed in the far-field measurement setup using a polarizer.[27] In addition, the light was propagated from one nanowire end with a specific angle in the *xy*-plane. In the TE-like mode, the angle between the light propagation and the nanowire axis was ~55°, unfortunately the directional emission along the nanowire axis could not be determined. This property is not advantageous for efficient light collection to the optical fibers or waveguides.[28,30] In order to use the nanowire as a practical light source, output photons should be efficiently coupled to the waveguide structures.[10] This is especially true when the nanowire constitutes a single photon source or a photonic integrated circuit; thus this critical issue should be addressed for improvement.[30] We are currently investigating the efficient coupling of the nanowire to an optical fiber.

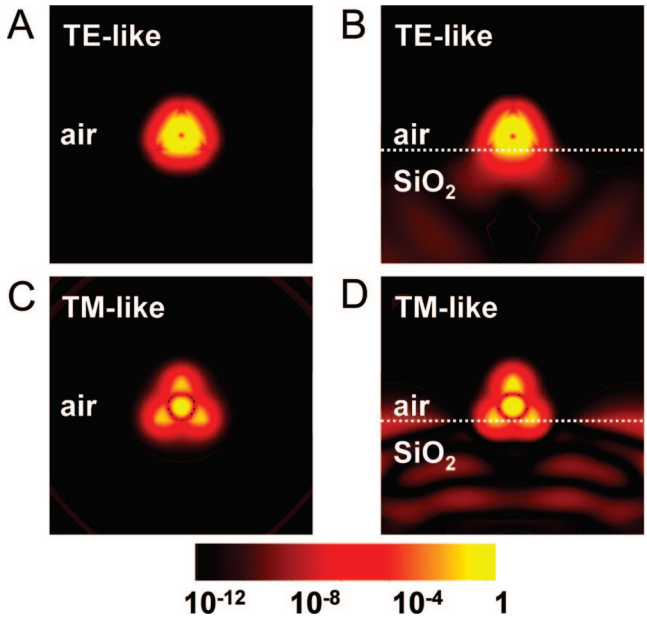

Figure 5. Electric field profiles (cross section) of the TE-like and the TM-like modes in the nanowire cavity with and without SiO_2 substrate. (A), C) The TE-like and the TM-like mode profiles without the substrate. (B), D) The TE-like and the TM-like mode profiles with the substrate.

Finally, we examined a more realistic case, a nanowire on a SiO_2 substrate, since it is known that a substrate can severely affect the optical properties of a nanowire. 3-D FDTD computations were performed in a nanowire on a SiO_2 substrate with a refractive index of 1.5 (Figure 5 and Supporting Information). As shown in Figure 5, more serious optical losses were observed in the TM-like mode as a result of the substrate. Less light escaped through the substrate in the case of the TE-like mode; thus, we expect that the TE-like mode could be more effectively lased. In Figures S2 and S3 in the Supporting Information, *Q* factors, confinement factors, and dispersion curves were calculated when the SiO_2 substrate was introduced underneath the single-GaN nanowire. Although the highest *Q* factor of the fundamental TE-like mode was reduced in this case, the confinement factor (>0.9) was still large enough to support lasing.[6] However, additional transverse resonant modes were introduced in the nanowire located on the substrate as shown in the dispersion curves (Figure S3). Light emission from the nanowire interacts with the substrate; hence, the single-mode region was slightly reduced.

In summary, we have investigated modal characteristics of a single-GaN nanowire cavity with a triangular cross section through theoretical analysis. Optical properties such as *Q* factors, confinement factors, and single-mode conditions for the TE-like and the TM-like transverse modes were determined using 3-D FDTD simulation. In addition, far-field emission properties were analyzed, which could be compared with experimental measurements. These FDTD simulation results provide a significant step toward the design of high-*Q*, single-mode, low-threshold nanowire lasers suitable for ultracompact nanoscale photonic integrated circuits.

Acknowledgment. This work was supported by Grant No. (R11-2003-022) from OPERA of the Korea Science and Engineering Foundation and the Seoul R & BD Program.

Supporting Information Available: Light in vs light out obtained from the rate equation analysis; *Q* and confinement factors of the TE-like and the TM-like modes in a nanowire cavity located on SiO_2 substrate; dispersion curves in a nanowire cavity located on a SiO_2 substrate. This material is available free of charge via the Internet at http://pubs.acs.org.

References

(1) Lieber, C. M.; Wang, Z. L. *Mater. Res. Soc. Bull.* **2007**, *32*, 99–104.
(2) Huang, M. H.; Mao, S.; Feick, H.; Yan, H. Q.; Wu, Y. Y.; Kind, H.; Weber, E.; Russo, R.; Yang, P. D. *Science* **2001**, *292*, 1897–1899.
(3) Johnson, J. C.; Choi, H. J.; Knutsen, K. P.; Schaller, R. D.; Yang, P. D.; Saykally, R. J. *Nat. Mater.* **2002**, *1*, 106–110.
(4) Duan, X.; Huang, Y.; Agarwal, R.; Lieber, C. M. *Nature* **2003**, *421*, 241–245.
(5) Huang, Y.; Duan, X.; Lieber, C. M. *Small* **2005**, *1*, 142–147.
(6) Gradecak, S.; Qian, F.; Li, Y.; Park, H.-G.; Lieber, C. M. *Appl. Phys. Lett.* **2005**, *87*, 173111.
(7) Qian, F.; Gradecak, S.; Li, Y.; Wen, C.-Y.; Lieber, C. M. *Nano Lett.* **2005**, *5*, 2287–2291.
(8) Barrelet, C. J.; Greytak, A. B.; Lieber, C. M. *Nano Lett.* **2004**, *4*, 1981–1985.
(9) Barrelet, C. J.; Bao, J.; Loncar, M.; Park, H.-G.; Capasso, F.; Lieber, C. M. *Nano Lett.* **2006**, *6*, 11–15.
(10) Park, H.-G.; Barrelet, C. J.; Wu, Y.; Tian, B.; Qian, F.; Lieber, C. M. *Nat. Photonics* **2008**, *2*, 622−626.
(11) Park, H.-G.; Qian, F.; Barrelet, C. J.; Li, Y. *Appl. Phys. Lett.* **2007**, *91*, 251115.
(12) Maslov, A. V.; Ning, C. Z. *Opt. Lett.* **2004**, *29*, 572–574.
(13) Wang, M.-Q.; Huang, Y.-Z.; Chen, Q.; Cai, Z.-P. *IEEE J. Quantum Electron.* **2006**, *42*, 146–151.
(14) Maslov, A. V.; Ning, C. Z. *Appl. Phys. Lett.* **2003**, *83*, 1237–1239.
(15) Chen, L.; Towe, E. *Appl. Phys. Lett.* **2006**, *89*, 053125.
(16) Chen, L.; Towe, E. *J. Appl. Phys.* **2006**, *100*, 044305.
(17) Taflove, A.; Hagness, S. C. *Computational electrodynamics: The finite-difference time-domain method*; Artech House: London, 2000.
(18) Yariv, A. *Optical electronics in modern communication*; Oxford University Press: Oxford, 1997.
(19) Park, H.-G.; Hwang, J.-K.; Huh, J.; Ryu, H.-Y.; Kim, S.-H.; Kim, J.-S.; Lee, Y.-H. *IEEE J. Quantum Electron.* **2002**, *38*, 1353–1365.
(20) Park, H.-G.; Kim, S.-H.; Kwon, S.-H.; Ju, Y.-G.; Yang, J.-K.; Baek, J.-H.; Kim, S.-B.; Lee, Y.-H. *Science* **2004**, *305*, 1444–1447.
(21) Tamboli, A. C.; Haberer, E. D.; Sharma, R.; Lee, K. H.; Nakamura, S.; Hu, E. L. *Nat. Photonics* **2006**, *1*, 61–64.
(22) Coldren, L. A.; Corzine, S. W. *Diode lasers and photonic integrated circuits*; John Wiley & Sons, Inc.: New York, 1995.
(23) Mackowiak, P.; Nakwaskiy, W. *J. Phys. D* **1998**, *31*, 2479–2484.
(24) Muth, J. F.; Lee, J. H.; Shmagin, I. K.; Kolbas, R. M.; Casey, H. C., Jr.; Keller, B. P.; Mishra, U. K.; DenBaars, S. P. *Appl. Phys. Lett.* **1997**, *71*, 2572–2574.
(25) Fang, Q.; Li, Y.; Gradecak, S.; Park, H.-G.; Dong, Y.; Wang, Z. L.; Lieber, C. M. *Nat. Mater.* **2008**, *7*, 701–706.
(26) Vuckovic, J.; Loncar, M.; Mabuchi, H.; Scherer, A. *IEEE J. Quantum Electron.* **2002**, *38*, 850–856.
(27) Shin, D.-J.; Kim, S.-H.; Hwang, J.-K.; Ryu, H.-Y.; Park, H.-G.; Song, D.-S.; Lee, Y.-H. *IEEE J. Quantum Electron.* **2002**, *38*, 857–866.
(28) Kim, S.-H.; Kim, S.-K.; Lee, Y.-H. *Phys. Rev. B* **2006**, *73*, 235117.
(29) The far-field emission pattern detected in a half sphere is redrawn in a two-dimensional (2-D) plane (*yz*-plane). In the concentric circle of Figure 4A (right side), the center of a circle is in the nanowire axis and the outer circle is normal to the nanowire. This mapping is useful to understand the complicated 3-D emission pattern.[26]
(30) Hwang, I.-K.; Kim, S.-K.; Yang, J.-K.; Kim, S.-H.; Lee, S. H.; Lee, Y.-H. *Appl. Phys. Lett.* **2005**, *87*, 131107.

NL8027125